

Ultrafiltration of Lignin from Black Liquor: Modelling Decline in Flux

P T Kekana^{1,2}, B B Sithole^{1,2*} and D Ramjugernath²

¹Biorefinery Industry Development Facility, Council for Scientific and Industrial Research, Durban,

²University of KwaZulu-Natal, Discipline of Chemical Engineering, King George V Avenue, Durban, ZA 4041

Received 02 February 2018; revised 17 June 2018; accepted 23 December 2018

Fundamental studies on membrane fouling caused by organic matter during ultrafiltration have been carried out widely by using the stirred dead-end filtration setup. In this study, black liquor ultrafiltration experiments have been carried out using a hydrophilic polyethersulfone membrane with a cut-off size of 10kDa in a stirred batch cell over a wide range of operating conditions. The effect of operating conditions (pressure, feed concentration and stirring rate) on transient flux profiles was studied in order to elucidate the fouling mechanism involved. Results indicated that the operating conditions have a significant effect on the flux decline behaviour. The solute mass balance for a stirred cell and the intermediate blocking model were applied to model the flux decline experimental data. The simulation results were compared to the experimental results and they were found to be in good agreement predominantly for filtration time that was ≥ 20 minutes.

Keywords: Flux Decline, Membrane, Fouling, Modelling, Ultrafiltration

Introduction

Ultra-filtration is a physical membrane separation process that uses pressure as the driving force to separate solutes in the molecular weight range of 5kDa to 500kDa^{1,2}. When ultrafiltration is applied to the pulp and paper industry it can be useful in the recovery of water as well as other valuable chemicals from the black liquor^{3,4}. The rising energy costs as well as the large quantities of water lost in the conventional recovery process justify the need for more economical, environmentally friendly alternatives for treating black liquor^{4,5}. A stirred cell is a convenient module that is used extensively for laboratory scale experiments to validate any concept of separation or performance of membrane for a particular application⁶. In batch mode operation, the feed concentration in the stirred cell increases with time as the volume decreases during the course of the filtration process. Thus it is important to develop a model that takes into account the variation of feed concentration and feed volume with time. Therefore the objective of this paper is to elucidate the fouling mechanism involved in the ultrafiltration of black liquor using polymeric membranes in a stirred cell as well as the development of a model that can be solved numerically to predict the flux decline with time during the course of the filtration process.

Stirred cell modelling theory

In this study it is assumed that the fouling mechanism encountered during filtration is described by the intermediate blocking model. With the intermediate blocking model it is assumed that foulants reaching the membrane directly block some membrane area or deposit on other already deposited fouling particles. The solute mass balance for a stirred cell was applied to model the flux decline experimental data and the total resistance was expressed using a resistance-in-series model based on Darcy's law. A model for constant pressure dead-end filtration laws was proposed to analyze the flux decline during ultrafiltration in a batch cell⁶. The proposed model was based on Hermia's classic filtration laws and sequential occurrence of complete pore blocking and cake filtration mechanisms and the modelling procedure used by the author was adapted for this study. However, in this study only one mechanism (intermediate blocking) was considered as opposed to the two mechanisms considered by the author⁶. The governing equation of flux decline due to pore blocking for constant pressure filtration can be represented in dimensionless form as:

$$F(\tau) = \frac{F_0}{k_1 F_0 \tau + 1} \quad \dots (1)$$

Where $k_1 = k_i R$; $F_0 = \frac{J_0 R}{D}$ and $J_0 = \Delta P / \mu R_m$ is the initial permeate flux

*Author for Correspondence
E-mail: bsithole@csir.co.za

The membrane hydraulic resistance as well as the intermediate fouling can be considered as two resistances in series of a resistance-in-series model based on Darcy's law. The filtration rate J is related to the filtration resistance and transmembrane pressure as⁶:

$$J = \frac{\Delta P}{\mu_p R_t} = \frac{\Delta P}{\mu(R_m + R_i)} \quad \dots (2)$$

In dimensionless form Equation (2) can be written as⁶:

$$F(\tau) = \frac{F_0}{1 + R_{id}} \quad \dots (3)$$

Where R_{id} is the dimensionless intermediate resistance. R_{id} is expressed in terms of intermediate blocking resistance R_i and membrane hydraulic resistance R_m as $R_{id} = R_i/R_m$

From Equations (1) and (3), the dimensionless intermediate resistance R_{id} can be expressed as:

$$R_{id} = k_1 F_0 \tau \quad \dots (4)$$

Materials and methods

Materials

Black liquor was procured from a South African eucalyptus Kraft mill. The black liquor was diluted with deionised water to get the desired concentrations. A hydrophilic polyether sulfone membrane with a molecular cut-off size of 10 kDa was procured from Memcon (Pty) Ltd, South Africa. The membrane is usable in the pH range 0-14 and are resistant to temperatures up to 95°C. The composition of the black liquor used is reported in Table 1 below.

Apparatus

A stirred dead-end filtration configuration was employed for the ultrafiltration experiments. The

stirred cell (Amicon 8400, Merck, South Africa) had a volume of 400 mL and a diameter of 76 mm. The cell was connected to a compressed air cylinder and the pressure in the cell was controlled by adjusting the pressure regulator on the outlet side of the cylinder and monitored by a calibrated pressure gauge on the inlet of the cell. The effective filtration area of the cell is 41.8 cm² and the clearance between the flat stirrer hanging from the top inside the cell and the membrane is 1.5 mm. Stirring inside the cell was accomplished by utilizing a magnetic stirrer with a digital display (MS-H280-Pro, Scilogex, USA). A constant temperature in the cell during operation was achieved by means of a heating copper coil inserted around the stirred cell body. Water from a heating bath was circulated in the heating coil using a peristaltic pump (323, Watson Marlow, South Africa).

Analysis

The total dissolved solids (TDS) concentrations were determined gravimetrically by evaporating a known volume of black liquor sample at 105°C for 24 hours and determining the weight of the residue. Lignin can be measured from the light absorption at a wavelength of 280 nm as it contains phenolic groups which absorb light. A UV-Visible spectrophotometer (Varian CARY 50 CONC) was used to measure the UV light absorption of the black liquor samples. The samples were diluted with 0.1 M NaOH and an absorption constant of 24.6 L/g cm was used. The hemicelluloses content of the black liquor was determined using a High Performance Liquid Chromatography, comprising an autosampler (Perkin Elmer, Series 200), column oven (Perkin Elmer, Series 200), chromatography interface (Perkin Elmer, 600 Series), pulsed amperometric detector (Dionex) and analytical column (CarboPac PA-1, Dionex)

Ultrafiltration procedure

Ultrafiltration experiments were carried out to investigate the effect of three variables; transmembrane pressure (150, 250 and 350 kPa), stirring rate (200, 300 and 400 rpm) and feed concentration (3, 6 and 9 m/m %) on lignin rejection and transient flux decline. One parameter was varied as the others were held constant to get an exact picture on dependence. All experiments were conducted at 60°C by circulating a heating water stream at 95°C and 15 rpm in the coil around the stirred cell body. The disk membrane was placed on the porous support and the cell was assembled. Pure

Table — 1 Composition of the raw black liquor

Lignin (g/L)	44.02
Total solids content (g/L)	121.72
Ash (% m/m)	9.02
Hemicelluloses (% m/m)	
Xylose	0.03
Arabinose	0.15
Galactose	0.03
Mannose	0.00
Glucose	0.00

water flux at different transmembrane pressures was measured and plotted against the transmembrane pressure. The membrane resistance for the 10 kDa membrane was calculated from the slope of this plot. This was followed by the actual experiment by charging the cell with 200 mL of black liquor solution. The transmembrane pressure and stirrer speed were adjusted to desired levels using a pressure regulator and the speed controller on the magnetic stirrer, respectively. The duration of each experiment was 1 hour and permeate at different time intervals was measured by collecting 10 mL of permeate in a measuring cylinder and recording the time for this collection. The retentate was collected by opening the stirred cell after each run. After each run, the cell was dismantled and the membrane thoroughly washed with deionised water to remove any deposition. The membrane was soaked in distilled water overnight and pure water flux was checked again to observe any variation in its hydraulic resistance before its reuse. This procedure was repeated after every experiment

Results and Discussions

Table 2 represents the intermediate blocking constant (k_i) values estimated from the simulation work. The dependence of the k_i values on experimental parameters under different operating conditions is discussed in subsequent sections. The error between the experimental and calculated values ranged from 1% to 8%. (Table 2) To study the fouling mechanism at different transmembrane pressures of 150, 250 and 350 kPa, the feed concentration and stirring rate were fixed at 3% and 200 rpm, respectively. From Table 2, the k_i values were found to decrease with an increase in transmembrane

pressure. For example, as shown in Table 2, an increase in transmembrane pressure from 150 to 350 kPa resulted in a decrease in k_i from 87.21-65.79 m^{-1} . The decrease in the resistance coefficient k_i could be attributed to the increase in driving force of solvent through the membrane which resulted in higher initial permeate flux values at higher pressures. This was also observed for the ultrafiltration of a polysaccharide in a stirred cell⁶. In the study the author observed that increasing the transmembrane pressure resulted in a decrease in the cake filtration constant, k_c , albeit marginally so. The author attributed this to the fact that the effect of pressure is marginal on the long term flux in a system whereby the cake filtration mechanism is dominating. The k_i values for different feed concentrations of 3, 6 and 9% are also shown in Table. 2. These are plotted for fixed transmembrane pressure and stirring rate values of 250 kPa and 300 rpm, respectively. The k_i values increase with an increase in feed concentration in the range investigated. For instance, as the feed concentration is increased from 3% to 9% (, the k_i values increase from 57.89-63.16 m^{-1} . This is an indication of an increase in concentration polarization which is as a result of the increase in solute feed concentration^{6,7}. This was also observed by other researchers^{8,9}, and the authors attributed this to the increase in membrane surface concentration leading to an increase in osmotic pressure which has a negative effect of the permeate flux. The k_i values for different stirring rates of 200, 300 and 400rpm are presented in Table 2. For this study the transmembrane pressure and feed concentration values were fixed at 250 kPa and 3%, respectively. The k_i values were found to decrease with an increase in stirring rate in the stirred cell. For example, an increase in stirring rate from 200 rpm to 400 rpm led to a decrease in k_i from 78.98-47.37 m^{-1} . This is attributed to the fact that at higher stirring rates there is enhanced turbulence close to the membrane surface which decreases concentration polarization and increases permeate flux⁶. The variation of dimensionless intermediate resistance with time for different transmembrane pressures is displayed in Figure. 1. For this study the feed concentration and stirring rate were fixed at 6% and 200 rpm, respectively. As shown in Figure. 1, the dimensionless intermediate resistance increases with an increase in transmembrane pressure. At the end of the experiment the dimensionless resistance increased

Table 2 — Estimated intermediate blocking model plugging constant under various experimental conditions

Operating conditions		Intermediate blocking law of Hermia
		$K_i (m^{-1})$
$C_o = 3\%$ $\omega = 200$ rpm	$\Delta P = 150$ kPa	84.21
	$\Delta P = 250$ kPa	78.95
	$\Delta P = 350$ kPa	65.79
$\Delta P = 250$ kPa $C_o = 3\%$	$\omega = 200$ rpm	78.95
	$\omega = 300$ rpm	52.63
	$\omega = 400$ rpm	47.37
$\Delta P = 250$ kPa $\omega = 300$ rpm	$C_o = 3\%$	57.89
	$C_o = 6\%$	60.53
	$C_o = 9\%$	63.16

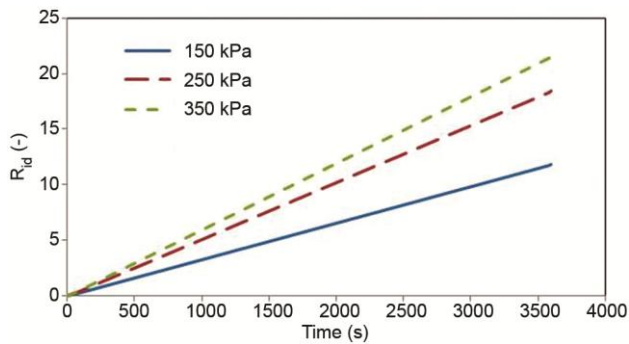


Fig — 1 Variation of dimensionless intermediate resistance with time at different transmembrane pressure. $C_o = 6\%$ and $\omega = 200$ rpm

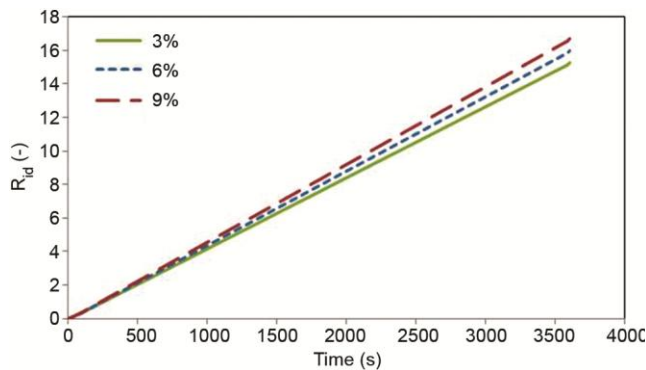


Fig — 2 Variation of dimensionless intermediate resistance with time at different feed concentration. $\Delta P = 250$ kPa and $\omega = 300$ rpm

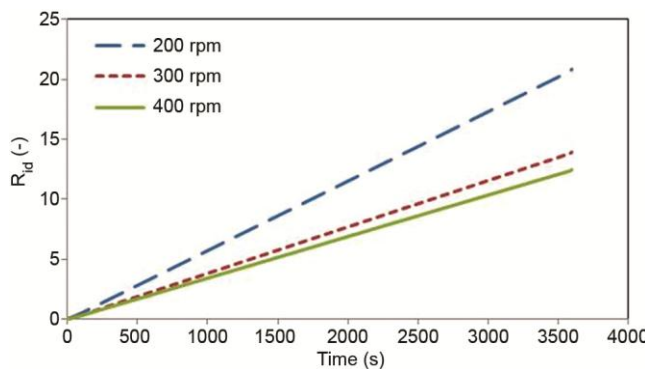


Fig — 3 Variation of dimensionless intermediate resistance with time at different stirring rates. $\Delta P = 250$ kPa and $C_o = 3\%$

from 11.83 to 21.56 with a corresponding increase in transmembrane pressure from 150 to 350 kPa. This is due to the fact that there is a higher convection of solutes to the membrane surface as the transmembrane pressure is increased which leads to increased concentration polarization at the surface as the thickness of the fouling layer increases⁶. Additionally the increase in membrane surface

concentration brought about by the increase in pressure could increase the osmotic pressure of the solution at the membrane surface thereby leading to a reduction in the net driving force to the transport of solutes⁸. Figure 2 represents the variation of dimensionless intermediate resistance with time at different feed concentration for fixed transmembrane pressure and stirring rate of 250 kPa and 300 rpm, respectively. An increase in the feed concentration led to an increase in the dimensionless intermediate resistance as shown in Figure. 2. For instance, at the end of the experiment, an increase in feed concentration from 3 to 9% resulted in a corresponding increase in the dimensionless intermediate resistance from 15.28 to 16.67. A possible explanation for this observation is that in principle, an increase in feed concentration leads to a corresponding increase in concentration polarization as the fouling layer on the membrane surface is increased.^{7,8} However, it is worth noting that the effect of feed concentration on the dimensionless intermediate resistance is marginal as compared to the effect of transmembrane pressure as shown in the preceding section. (Figure 2) The variation of dimensionless intermediate resistance with time at different stirring rates at fixed transmembrane pressure and feed concentrations of 250 kPa and 3% is shown in Figure. 3. From Figure. 3, it can be observed that an increase in the stirring rate resulted in a decrease in the dimensionless intermediate resistance. At the end of the experiment, the intermediate resistance was reduced significantly from 20.84 to 13.89 as the stirring rate was adjusted from 200 to 300 rpm, only to be reduced marginally to 12.50 as the stirring rate was further adjusted to 400 rpm. This is because at higher stirring rates, the enhanced turbulence close to the membrane surface assists in the mitigation of the effects of concentration polarization which leads to an enhancement in flux^{6,7,9}.

Conclusions

An ultrafiltration study has been conducted to investigate the effect of operating conditions on the flux decline behaviour of black liquor in a dead-end stirred cell in order to elucidate the fouling mechanism involved. From the results it was observed that the operating conditions had a significant effect on the retardation or exacerbation of concentration polarization which in turn had an effect on the transient flux profiles obtained. Increases in pressure and feed concentration were found to worsen the fouling on the

membrane surface while on the other hand an increase in stirring rate in the stirred cell was found to mitigate the onset of fouling. The results were modelled by solving differential equations of the solute mass balance in the stirred cell with the intermediate blocking model which was used to describe the fouling mechanism observed in the study. The intermediate blocking constant k_i , estimated from the simulation work was also used to explain the effect of operating conditions on the flux behaviour of the black liquor to corroborate theoretical explanations as well as similar results obtained by other researchers. For filtration time of 20 minutes and beyond the simulation results agreed well with the experimental results.

Nomenclature

D	Solute diffusivity (m^2/s)
F	permeate flux (dimensionless)
F_0	Pure water flux (dimensionless)
J	Permeate flux ($\text{m}^3/\text{m}^2\text{s}$)
J_0	Initial permeate flux ($\text{m}^3/\text{m}^2\text{s}$)
k_i	Intermediate blocking constant (m^{-1})
k_1	Parameter in Equation (1) (dimensionless)
R	Radius of cell (m)
R_{id}	Dimensionless intermediate resistance expressed in terms of intermediate blocking resistance
R_i	and membrane hydraulic resistance R_m as $R_{id} = R_i/R_m$
R_i	Intermediate blocking resistance (m^{-1})
R_m	Membrane hydraulic resistance (m^{-1})
t	Time (s)
<i>Greek letters</i>	
μ	Viscosity (Pa s)
τ	Characteristic time constant defined as $\tau =$

tD/R^2 (dimensionless)

ΔP Transmembrane pressure difference (kPa)

Subscripts

d dimensionless

0 initial condition

References

- 1 Kekana P, Sithole B & Ramjugernath D, Stirred cell ultrafiltration of lignin from black liquor generated from South African kraft mills, *S Afr J Sci*, **112(11/12)** (2016) Art. #2015-0280, 7 pages. <http://dx.doi.org/10.17159/sajs.2016/20150280>
- 2 Yobilishetty S M & Marathe K V, Removal of molybdenum (VI) from effluent waste water streams by cross flow micellar enhanced ultrafiltration (MEUF) using anionic, non-ionic and mixed surfactants, *IJCT*, **21(5-6)** (2014) 321-327
- 3 Nikita S K, Meisha L S & Sankar N, Membranes for Kraft black liquor concentration and chemical recovery: Current progress, challenges, and opportunities, *Sep Sci Technol*, **52:6** (2017) 1070-1094, DOI: 10.1080/01496395.2017.1279180
- 4 Darmawan A, Hardi F, Yoshikawa K, Aziz M & Tokimatsu K, Electricity production from black liquor: a novel integrated system, *Energy Procedia*, **142** (2017) 23-28
- 5 Huet M, Roubaud A, Chirat C & Lachenal D, Hydrothermal treatment of black liquor for energy and phenolic platform molecules recovery in a pulp mill, *Biomass and Bioenergy*, **89** (2016) 105-112
- 6 Sarkar B A, A combined complete pore blocking and cake filtration model during ultrafiltration of polysaccharide in a batch cell, *J Food Eng*, **116** (2013) 333-343
- 7 Banerjee S & De S, An analytical solution of Sherwood number in a stirred continuous cell during steady state ultrafiltration, *J Membr Sci*, **389**(2012) 188-196
- 8 De S & Bhattacharya P K, Flux prediction of black liquor in cross flow ultrafiltration using low and high rejecting membranes, *J Membr Sci*, **109** (1996) 109-123
- 9 Satyanarayana S V, Bhattacharya P K & De S, Flux decline during ultrafiltration of kraft black liquor using different flow modules: a comparative study, *Sep Purif Technol*, **20** (2000) 155-167